

Protecting spin squeezing from decoherence

Lin Jiao,¹ Han Pu,^{1,*} and Jun-Hong An^{2,†}

¹*Department of Physics and Astronomy, and Smalley-Curl Institute,
Rice University, Houston, TX 77251-1892, USA*

²*Key Laboratory of Quantum Theory and Applications of MoE,
Lanzhou Center for Theoretical Physics, Key Laboratory of Theoretical Physics of Gansu Province,
Gansu Provincial Research Center for Basic Disciplines of Quantum Physics, Lanzhou University, Lanzhou 730000, China*

As a crucial resource in the field of quantum metrology, spin squeezing can facilitate highly precise measurements that surpass the limitations imposed by classical physics. However, the quantum advantages of spin squeezing can be significantly compromised by decoherence, thereby impeding its practical implementation. Here, by investigating the influence of local dissipative environment on spin squeezing beyond the conventional Born-Markov approximation, we find a mechanism to protect spin squeezing from decoherence and show that robust spin squeezing can be achieved in the steady state. We outline an experimental proposal to verify our prediction in a trapped-ion platform. Overcoming the challenges set by decoherence on spin squeezing, our work provides a guideline for realizing high-precision sensing in realistic environments.

Introduction — The goal of quantum metrology is to achieve higher precision in measurements than is classically feasible by exploiting quantum resources, and as such it is expected to bring a number of significant technological breakthroughs [1, 2]. One such distinguished quantum resource is spin squeezing, which is closely related to many-body entanglement [3]. As a consequence of quantum correlations between particles, spin-squeezed states exhibit reduced quantum fluctuations of collective spins [3–7] in comparison to uncorrelated spin coherent states, thus holding promise for the development of next-generation revolutionary technologies, such as quantum gyroscope and gravimetry [8–11], atomic clocks [12–17], and magnetometers [18–21]. Recent experimental advances have realized spin squeezing in atomic ensembles comprising up to 10^{13} atoms [20, 22, 23].

As in most quantum resources, the practical application of spin squeezing in large-scale quantum metrology is challenged by decoherence caused by various kinds of noise in the quantum world. Spin squeezing tends to deteriorate or even completely vanish under the influence of decoherence [24–27], limiting both its stability [28] and scalability [29–31]. Therefore, developing efficient strategies to protect spin squeezing from decoherence is of crucial importance. Active ways, including dynamical decoupling [32], weak measurement [33], and reservoir engineering [34], have been proposed to overcome the destructive effects of decoherence on spin squeezing. A common character of these works is that the description of decoherence was based on the Born-Markov approximation. Given the inherent non-Markovian nature of the decoherence dynamics [35–38], however, such a treatment may not be sufficient. In fact, the non-Markovian effect was found to play a positive role in preserving the quantum advantages of optical squeezing [39] and GHZ-type entanglement [40–42] in noisy quantum metrology. It is therefore important to investigate the effects of non-Markovian baths on spin squeezing.

In this work, by investigating the non-Markovian decoherence dynamics of an atomic ensemble prepared in spin squeezed states, we find that the stability and scalability of the spin squeezing are essentially determined by the feature of the energy spectrum of the total system formed by each atom and its local environment. Contrary to conventional wisdom, it is found that a sufficiently strong system-bath coupling may help to preserve spin squeezing. We propose testing this prediction on a trapped-ion platform. Our work provides a universal mechanism for realizing stable and scalable spin squeezing, crucial for high-precision quantum metrology in realistic noisy environments.

Spin squeezing — Spin squeezed states are entangled states of collective spins whose uncertainty in certain spin components perpendicular to the mean spin direction is reduced below that of a spin coherent state. Consider that an ensemble of N two-level atoms or spin-1/2 particles described by the Pauli matrices $\hat{\sigma}_l = (\hat{\sigma}_l^x, \hat{\sigma}_l^y, \hat{\sigma}_l^z)$, with $l = 1, \dots, N$, is in a state ρ . The mean spin direction of ρ is defined as $\mathbf{n}_0 = \langle \hat{\mathbf{J}} \rangle / |\langle \hat{\mathbf{J}} \rangle|$, where $\langle \hat{\mathbf{J}} \rangle = \text{Tr}(\rho \hat{\mathbf{J}})$ and $\hat{\mathbf{J}} = 1/2 \sum_{l=1}^N \hat{\sigma}_l$ is the collective spin. It is well established that when using such a state to measure a phase ϕ in the Ramsey spectroscopy, the obtained phase-estimation error is $\delta\phi = \min_{\beta} \Delta J_{\perp, \beta} / |\langle \hat{\mathbf{J}} \rangle|$ [4], where $\Delta J_{\perp, \beta} = (\langle \hat{J}_{\perp, \beta}^2 \rangle - \langle \hat{J}_{\perp, \beta} \rangle^2)^{1/2}$ is the uncertainty of the spin component $\hat{J}_{\perp, \beta} = (\cos \beta \mathbf{n}_1 + \sin \beta \mathbf{n}_2) \cdot \hat{\mathbf{J}}$, with $\mathbf{n}_{1,2}$ being two orthogonal unit vectors perpendicular to \mathbf{n}_0 . For a spin coherent state given by $|\theta, \varphi\rangle = \frac{e^{i\zeta \hat{J}_-}}{(1+|\zeta|^2)^{j/2}} |j, j\rangle$, with $\zeta = e^{i\varphi} \tan \frac{\theta}{2}$, $\hat{J}_{\pm} = \hat{J}_x \pm i\hat{J}_y$, $j = N/2$, and $|j, j\rangle$ being the common eigenstate of \hat{J}^2 and \hat{J}_z , the phase-estimation error is $\delta\phi_{\text{SCS}} = N^{-1/2}$, which corresponds to the standard shot-noise limit (SNL). This motivated Wineland and coworkers to define $\xi \equiv \sqrt{N} \min_{\beta} \Delta J_{\perp, \beta} / |\langle \hat{\mathbf{J}} \rangle|$ as the spin squeezing parameter [6]. If $\xi < 1$, the state is spin squeezed and the phase-estimation error $\delta\phi = \xi / \sqrt{N}$

surpasses the SNL.

Two types of spin squeezed states, the so-called one-axis twisted (OAT) and two-axis twisted (TAT) states, are widely studied [43–49]. Both of them have their mean spin direction along the z -axis, and are generated from state $|j, -j\rangle$ as:

$$|\Psi_{\text{OAT}}\rangle = e^{-i\Theta \hat{J}_x^2} |j, -j\rangle, \quad (1)$$

$$|\Psi_{\text{TAT}}\rangle = e^{i\Theta(\hat{J}_+^2 - \hat{J}_-^2)} |j, -j\rangle. \quad (2)$$

The OAT state has been experimentally generated in systems of cold atoms [47, 48, 50, 51], trapped ions [52–54], and superconducting qubits [55–57]. For this state, it is straightforward to show that $\langle \hat{\mathbf{J}} \rangle = -j \cos^{2j-1} \Theta (0, 0, 1)$ and thus $\min_{\beta} \Delta J_{\perp, \beta}^2 = (\langle \hat{J}_x^2 + \hat{J}_y^2 \rangle - |\langle \hat{J}_z \rangle|^2)/2$. Taking advantage of the permutation symmetry between the N identical spins, we have

$$\begin{aligned} \langle \hat{J}_\alpha^2 \rangle &= N[1 + (N-1)\langle \hat{\sigma}_1^\alpha \hat{\sigma}_2^\alpha \rangle]/4, \\ \langle \hat{J}_z^2 \rangle &= N(N-1)\langle \hat{\sigma}_1 \hat{\sigma}_2 \rangle, \end{aligned}$$

with $\hat{\sigma}_l \equiv (\hat{\sigma}_l^x - i\hat{\sigma}_l^y)/2$. One can easily obtain $\langle \hat{\sigma}_1 \hat{\sigma}_2^\dagger \rangle = A/8$ and $\langle \hat{\sigma}_1 \hat{\sigma}_2 \rangle = -(A-iB)/8$, with $A \equiv 1 - \cos^{N-2}(2\Theta)$ and $B \equiv 4 \sin \Theta \cos^{N-2} \Theta$. It then follows that

$$\xi_{\text{OAT}}^2 \simeq 1 + (N-1)(A - \sqrt{A^2 + B^2})/4. \quad (3)$$

Under the condition $N\Theta^2 \ll 1 \ll N\Theta$, Eq. (3) tends to $\xi_{\text{OAT}}^2 \simeq (N\Theta)^{-2} + N^2\Theta^4/6$, which reaches its minimum value $\min \xi_{\text{OAT}}^2 \simeq 1.04N^{-2/3}$ when $\Theta = \Theta_0 \equiv 3^{1/6}/N^{2/3}$. Therefore, we achieve a phase estimation error $\delta\phi_{\text{OAT}} \propto N^{-5/6}$ using $|\Psi_{\text{OAT}}\rangle$ in Ramsey spectroscopy.

The squeezing properties of the TAT states are less analytically tractable. Through numerical fitting, it can be shown that the corresponding spin squeezing parameter scales with the atom number N as $\xi_{\text{TAT}} \simeq \sqrt{2}N^{-1/2}$ in the large- N limit. It implies that the phase-estimation error converges to the Heisenberg limit $\delta\phi_{\text{TAT}} \simeq \sqrt{2}N^{-1}$. Several theoretical schemes have been proposed to transform the one-axis twisting interaction into a two-axis one [58–62].

Effects of environment — The quantum advantages of using spin squeezing in quantum metrology are challenged by the decoherence caused by the inevitable interactions of systems with their environments. It has been found that the system-environment interplay caused by the inherent non-Markovian nature can induce diverse characters absent in the Born-Markov approximation [36, 38, 63–65]. To reveal the practical performance of spin squeezing in Ramsey spectroscopy, we go beyond the widely used Born-Markov approximation and investigate the impact of dissipative decoherence on spin squeezing.

We consider each spin coupled to their own dissipative environment. The Hamiltonian of the total system is $\hat{H} = \sum_{l=1}^N \hat{H}_l$ with

$$\hat{H}_l = \omega_0 \hat{\sigma}_l^\dagger \hat{\sigma}_l + \sum_k [\omega_k \hat{a}_{lk}^\dagger \hat{a}_{lk} + (g_{lk} \hat{a}_{lk} \hat{\sigma}_l^\dagger + \text{h.c.})], \quad (4)$$

where \hat{a}_{lk} is the annihilation operator of the k th mode with a frequency ω_k of the environment felt by the l th spin. Under the continuum limit, the spectral density of the environment is related to the coupling strength g_{lk} as $J_l(\omega) = \sum_k |g_{lk}|^2 \delta(\omega - \omega_{lk})$. We assume that the environments coupled to different spins are independent from each other and possess a common Ohmic-family spectral density $J_l(\omega) \equiv J(\omega) = \eta \omega^s \omega_c^{1-s} e^{-\omega/\omega_c}$, where η is a dimensionless quantity characterizing the spin-environment coupling strength, ω_c a cutoff frequency, and s the Ohmicity index. Under the initial condition that the N independent environments are in vacuum states, we can exactly trace the degrees of freedom of the environments from the unitary dynamics governed by Eq. (4) and obtain a non-Markovian master equation for the reduced density operator of the system

$$\dot{\rho}(t) = \sum_{l=1}^N \{-i\Omega(t)[\hat{\sigma}_l^\dagger \hat{\sigma}_l, \rho(t)] + \Gamma(t)\check{\mathcal{L}}_l \rho(t)\}, \quad (5)$$

where $\check{\mathcal{L}}_l \rho(t) = 2\hat{\sigma}_l \rho(t) \hat{\sigma}_l^\dagger - \{\hat{\sigma}_l^\dagger \hat{\sigma}_l, \rho(t)\}$ is the Lindblad superoperator and $\Gamma(t) + i\Omega(t) = -\dot{u}(t)/u(t)$, with $u(t)$ determined by

$$\dot{u}(t) + i\omega_0 u(t) + \int_0^t f(t-\tau)u(\tau)d\tau = 0, \quad (6)$$

with $u(0) = 1$, and $f(t-\tau) = \int_0^\infty J(\omega) e^{-i\omega(t-\tau)} d\omega$ the environmental correlation function. Equation (6) indicates that all the non-Markovian effects have been self-consistently incorporated into the time-dependent coefficients. The solution of Eq. (5) can be formally expressed by the Kraus representation as $\rho(t) = \check{\Lambda}_t^{\otimes N} \rho(0)$, where the superoperator $\check{\Lambda}_t \cdot = \sum_{\mu=1}^2 \hat{K}_\mu(t) \cdot \hat{K}_\mu^\dagger(t)$ with $\hat{K}_1 = \text{diag}[u(t), 1]$ and $\hat{K}_2 = [1 - |u(t)|^2]^{1/2} \hat{\sigma}$ [66, 67]. Because the permutation symmetry of the N spins is preserved in the presence of local dissipation, we can still evaluate the expectation values of the collective spins by those of the bipartite operators $\langle \hat{\sigma}_1^\dagger \hat{\sigma}_2^\alpha \rangle = \text{Tr}[\hat{\sigma}_1^\dagger \hat{\sigma}_2^\alpha \check{\Lambda}_t^{\otimes 2} \rho(0)] = \langle (\check{\Lambda}_t^\dagger \hat{\sigma}^\alpha)^{\otimes 2} \rangle_0$, where $\langle \cdot \rangle_0 = \text{Tr}[\cdot \rho(0)]$.

Let us first consider the initial state for the system to be the OAT state such that $\rho(0) = |\Psi_{\text{OAT}}\rangle \langle \Psi_{\text{OAT}}|$. It is easy to calculate $\check{\Lambda}_t^\dagger \hat{\sigma} = u(t) \hat{\sigma}$, from which we obtain [67]

$$\xi_{\text{OAT}}^2(t) = 1 + |u(t)|^2 (N-1)(A - \sqrt{A^2 + B^2})/4. \quad (7)$$

In the case when the system-environment coupling is weak and the correlation time of the environment characterized by $f(t-\tau)$ is much shorter than the typical time scale of the spins, we can apply the Born-Markov approximation [68, 69], under which the solution of Eq. (6) reads $u_{\text{BMA}}(t) = e^{-[\kappa + i(\omega_0 + \Delta(\omega_0))]t}$ with $\kappa = \pi J(\omega_0)$, $\Delta(\omega_0) = \mathcal{P} \int_0^\infty \frac{J(\omega)}{\omega_0 - \omega} d\omega$, and \mathcal{P} being the Cauchy principal value. Substituting this into Eq. (7), we readily obtain that $\xi_{\text{OAT}}^2(t)$ exponentially increases to one with

a rate $2\kappa \propto \eta$, which indicates that the spin squeezing as a quantum resource is destroyed with time, and the stronger the system-environment coupling strength is, the faster it is destroyed. This result is consistent with Markovian schemes [69–71], where the decoherence destroys the quantum advantages and, hence, achieving high-precision quantum sensing in the practical noisy settings is hampered by decoherence.

Now let us go beyond the Born-Markov approximation. In the general non-Markovian case, Eq. (6) can only be solved numerically. However, its long-time asymptotic form is analytically available by the Laplace-transform method. The Laplace transform of Eq. (6) reads $\tilde{u}(z) = [z + i\omega_0 + \int_0^\infty \frac{J(\omega)d\omega}{z+i\omega} d\omega]^{-1}$. Then $u(t)$ can be obtained by performing the inverse Laplace transform to $\tilde{u}(z)$. This requires to find the poles of $\tilde{u}(z)$ from the equation $Y(E) = E$, where $E = iz$ and $Y(E) \equiv \omega_0 - \int_0^\infty \frac{J(\omega)}{\omega - E} d\omega$. It is interesting to find that the roots E of this pole equation are just the eigenenergies of the total system formed by each spin and its environment. To prove this, we write the eigenstate as $|\Phi\rangle = (c\hat{\sigma}_l^\dagger + \sum_k d_k \hat{a}_{lk}^\dagger)|g_l, \{0_k\}\rangle$ and insert it into the Schrödinger equation $\hat{H}_l|\Phi\rangle = E|\Phi\rangle$ and obtain the eigenenergy equation as $E = \omega_0 + \sum_k g_{lk}^2/(\omega_k - E) = 0$, which matches with the roots of the pole equation in the continuum limit. $Y(E)$ is ill-defined and oscillates rapidly between $\pm\infty$ in the regime $E > 0$ due to the divergence of the integrand in $Y(E)$. Thus, we obtain infinite roots E in this regime, which form a continuum energy band. In the regime $E < 0$, $Y(E)$ is a monotonic decreasing function of E . It has an isolated root E_b provided $Y(0) < 0$, which represents a bound state. Substituting these poles into the inverse Laplace transform, we obtain [67]

$$u(t) = Ze^{-iE_b t} + \int_0^\infty \mathcal{C}(E)e^{-iEt} dE, \quad (8)$$

where $Z = [1 + \int_0^\infty \frac{J(\omega)d\omega}{(E_b - \omega)^2}]^{-1}$ originates from the bound state and $\mathcal{C}(E) = J(E)/\{[E - \omega_0 - \Delta(E)]^2 + [\pi J(E)]^2\}$ from the continuum energy band. The second term of $u(t)$ tends to zero in the long-time limit due to out-of-phase interference. Thus, we have

$$\lim_{t \rightarrow \infty} u(t) = \begin{cases} 0; & \text{without bound state} \\ Ze^{-iE_b t}; & \text{with bound state} \end{cases} \quad (9)$$

For the Ohmic-family spectral density, the condition to form the bound state, i.e., $Y(0) < 0$, amounts to

$$\eta > \eta_c \equiv \omega_0/[\omega_c \gamma(s)], \quad (10)$$

with $\gamma(s)$ being the Gamma function.

Equation (9), together with Eq. (7), clearly indicates the important role that the bound state plays. In the absence of the bound state, $u(t)$ tends to zero and, hence, ξ_{OAT} asymptotically tends to one, just like under the

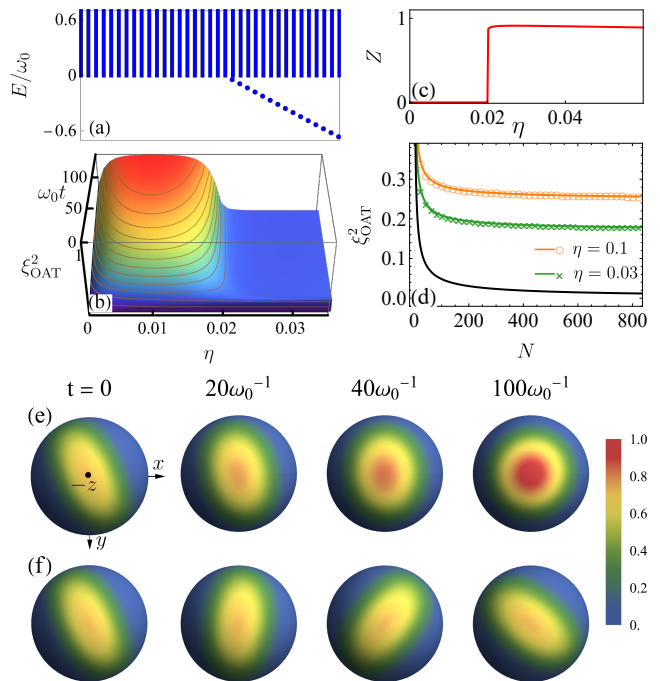


FIG. 1. (a) Energy spectrum of the composite spin-environment system and (b) evolution of $\xi_{\text{OAT}}^2(t)$ for $N = 100$. The brown solid lines represent the contour lines. (c) Z as a function of η . (d) $\xi_{\text{OAT}}^2(\infty)$ (evaluated at $t = 400\omega_0^{-1}$) as a function of N for several different η . Symbols are numerical results, while colored lines are analytic results from Eq. (11). The black line is the result in the ideal decoherence-free case. The inset shows $|u(t)|$ at $t = 400\omega_0^{-1}$ and Z . Normalized $Q(\theta, \varphi)$ at different time in the absence and presence of the bound state when $\eta = 0.01$ (e) and 0.03 (f) for $N = 10$. In all plots, we have $\omega_c = 50\omega_0$ and $s = 1$, which gives rise to a critical value $\eta_c = 0.02$ at which the bound state emerges. The initial state is $|\Psi_{\text{OAT}}\rangle$ in Eq. (1) with $\Theta = \Theta_0$ that optimizes the initial spin squeezing.

Born-Markov approximation. By contrast, in the presence of the bound state and for $N\Theta^2 \ll 1 \ll N\Theta$, we have $\xi_{\text{OAT}}^2(\infty) \simeq 1 + Z^2(N^{-2}\Theta^{-2} + N^2\Theta^4/6 - 1)$, which reaches its minimum

$$\xi_{\text{OAT}}^2(\infty)|_{\Theta=\Theta_0} \simeq 1.04Z^2N^{-\frac{2}{3}} + 1 - Z^2. \quad (11)$$

In the large N limit, we obtain the same N -scaling as in the ideal decoherence-free case. But here, ξ_{OAT} approaches a constant value $\sqrt{1 - Z^2}$. Thus, it is desirable to make Z as close to one as possible to achieve strong spin squeezing.

To verify our analytical results, we performed numerical calculations with the results shown in Fig. 1. Here we choose an Ohmic spectral density, i.e., $s = 1$. Qualitatively similar results are obtained for super- and sub-Ohmic spectral densities. We plot in Fig. 1(a) the energy spectrum of each spin and its local environment. We see that, for $\eta > \eta_c$, a bound state is formed. The evolution of $\xi_{\text{OAT}}^2(t)$, shown in Fig. 1(b), are obtained

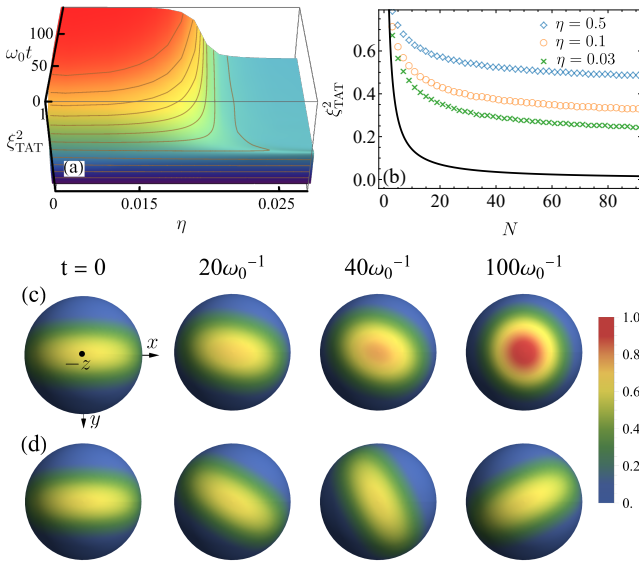


FIG. 2. (a) Evolution of $\xi_{\text{TAT}}^2(t)$ for $N = 50$. (b) Asymptotic value $\xi_{\text{TAT}}^2(\infty)$ as a function of N evaluated at $t = 400\omega_0^{-1}$. Normalized $Q(\theta, \varphi)$ at different times in the absence and presence of the bound state for $\eta = 0.01$ (c) and 0.03 (d) for $N = 10$. In all plots, we have $\omega_c = 50\omega_0$ and $s = 1$. The initial state is $|\Psi_{\text{TAT}}\rangle$ in Eq. (2) with a numerically obtained Θ that optimizes the initial spin squeezing.

from the exact numerical solution of Eq. (6). It confirms that when the bound state is absent, $\xi_{\text{OAT}}^2(t)$ approaches one; when the bound state is formed, $\xi_{\text{OAT}}^2(t)$ stabilizes at an η -dependent value less than one. This can also be observed in Fig. 1(c) where we plot Z as a function of η . When $\eta > \eta_c$, Z exhibits a sudden jump from 0 to a finite value, which reaches a maximum before gradually decreases. Choosing an sufficiently large t , we plot $\xi_{\text{OAT}}^2(\infty)$ as a function of the spin number N in Fig. 1(d). The numerical results and the analytic results of Eq. (11) are in perfect agreement. Finally, in order to visually depict the evolution of the spin squeezing, we plot in Figs. 1(e) and 1(f) the Husimi function $Q(\theta, \varphi) = (2j + 1)/(4\pi) \langle \theta, \varphi | \rho(t) | \theta, \varphi \rangle$, which maps $\rho(t)$ to a quasiclassical probability distribution in the phase space defined by the spin coherent state $|\theta, \varphi\rangle$ [67]. Figure 1(d) shows that, for $\eta < \eta_c$, spin squeezing gradually vanishes and the system tends to a spin coherent state with an isotropically distributed spin variance. For $\eta > \eta_c$, on the other hand, spin squeezing is preserved in the steady state, as shown in Fig. 1(f). The numerical result confirms the powerful role of the energy spectrum of the total system in determining the dynamics of the open system. The formation of the bound state offers us with a useful mechanism to protect the spin squeezing from the destruction of dissipative noise.

So far, we have discussed the effects of the environment on the OAT state $|\Psi_{\text{OAT}}\rangle$. Similar studies can be

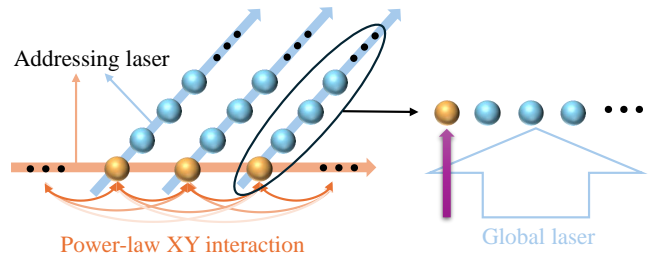


FIG. 3. An implementation of Eq. (4) on a trapped-ion platform. The edge ion chain (orange spheres) exhibits power-law XY interactions (orange lines) leading to the formation of a squeezed spin state. Each row of ions (blue spheres) confined by beams (blue arrows) act as an environment. A narrow beam (magenta arrow) is used to control the coupling between each edge ion and its environment.

carried out for the TAT state $|\Psi_{\text{TAT}}\rangle$ being the initial state. Using the Kraus representation, we can show

$$\xi_{\text{TAT}}^2(t) = 1 - |u(t)|^2 + \frac{2|u(t)|^2}{N} (\langle \hat{J}_x^2 + \hat{J}_y^2 \rangle_0 - |\langle \hat{J}_z \rangle_0|^2). \quad (12)$$

As in the case for $|\Psi_{\text{OAT}}\rangle$, $\xi_{\text{TAT}}^2(t)$ also tends to one under the Born-Markov approximation or in the absence of the bound state. As long as the bound state is formed, $\xi_{\text{TAT}}^2(t)$ tends to the asymptotic value $\xi_{\text{TAT}}^2(\infty)$ which has the same form as Eq. (12) but with $u(t)$ replaced by Z . In the large N limit, $\xi_{\text{TAT}}(\infty) = \sqrt{1 - Z^2}$ as in the case for OAT. The numerical results for the TAT state are shown in Fig. 2.

Experimental implementation — Let us now consider the possible experimental implementation. The bound state and its dynamical effect have been observed in circuit QED systems [72] and ultra-cold atom systems [73–75]. Spin squeezing in atomic ensembles has achieved levels of up to 20 dB [76], with free evolution times that extend up to 1 second [28]. The Ohmic spectral density can be effectively approximated by a sum of Lorentzian lines determined by the motional modes of the structured environment [77, 78]. Based on existing experimental evidence [79–81], we propose a feasible scheme utilizing a two-dimensional (2D) trapped-ion platform to verify our result, as sketched in Fig. 3. The efficient loading of a small 2D ion array has been experimentally demonstrated [81]. The 2D ion array consists of N 1D ion chains. The N ions at the end of each chain, depicted as the orange spheres in Fig. 3, form the spins of the system. These edge ions can be prepared in a spin squeezed state via a global addressing beam which induces power-law transverse-field Ising interactions between spins [79]. The rest of the ions in each chain serve as the environment for the corresponding edge ion, and together they realize the Hamiltonian (4) in each chain. A single chain governed by such a Hamiltonian was realized in a recent experiment [80], where it was also successfully shown that an

environment with effective Ohmic spectral density can be engineered. The experimental parameters can be tuned so that the condition for formation of the bound state can be met. These experimental advances provide strong supports for the realizability of our result.

Conclusion — In summary, we have demonstrated a non-Markovian mechanism to protect spin squeezing from a dissipative environment. Although we have modeled the environment with an Ohmic-family spectral density, we expect that this mechanism could also work for environments with other types of spectral densities. Note that previous studies have explored the non-Markovian effects of both individual [82, 83] and correlated [84, 85] decoherence on spin squeezing, but these works have not noticed the importance of the bound state discussed here and hence none of them achieves spin squeezing in the long time asymptotic limit. In contrast, in the current work we found that the dynamics of the spin squeezing for both the one- and two-axis twisted models depend sensitively on the feature of the energy spectrum of the total spin-environment system. Counterintuitively, to preserve spin squeezing, one needs to increase the system-environment coupling strength over a critical value such that the bound state is formed in the composite system. Accompanying the formation of the bound state, spin squeezing is preserved in the steady state. Our mechanism breaks the constraint of decoherence in quantum metrology and provides a guideline for developing high-precision quantum sensing using spin squeezing in the presence of practical dissipative noises using the technique of quantum reservoir engineering.

Acknowledgments — We acknowledge Si-Yuan Bai for the insightful discussions and Mingjian Zhu for suggestions. HP acknowledges support from U.S. NSF and the Welch Foundation (Grant No. C-1669). JHA is supported by the National Natural Science Foundation of China (Grants No. 12275109 and No. 12247101), the Innovation Program for Quantum Science and Technology of China (Grant No. 2023ZD0300904).

* hpu@rice.edu

† anjhong@lzu.edu.cn

- [1] C. L. Degen, F. Reinhard, and P. Cappellaro, Quantum sensing, *Rev. Mod. Phys.* **89**, 035002 (2017).
- [2] L. Pezzè, A. Smerzi, M. K. Oberthaler, R. Schmied, and P. Treutlein, Quantum metrology with nonclassical states of atomic ensembles, *Rev. Mod. Phys.* **90**, 035005 (2018).
- [3] B. Lücke, J. Peise, G. Vitagliano, J. Arlt, L. Santos, G. Tóth, and C. Klempt, Detecting multiparticle entanglement of Dicke states, *Phys. Rev. Lett.* **112**, 155304 (2014).
- [4] D. J. Wineland, J. J. Bollinger, W. M. Itano, F. L. Moore, and D. J. Heinzen, Spin squeezing and reduced quantum noise in spectroscopy, *Phys. Rev. A* **46**, R6797 (1992).
- [5] M. Kitagawa and M. Ueda, Squeezed spin states, *Phys. Rev. A* **47**, 5138 (1993).
- [6] D. J. Wineland, J. J. Bollinger, W. M. Itano, and D. J. Heinzen, Squeezed atomic states and projection noise in spectroscopy, *Phys. Rev. A* **50**, 67 (1994).
- [7] J. Ma, X. Wang, C. Sun, and F. Nori, Quantum spin squeezing, *Physics Reports* **509**, 89 (2011).
- [8] G. Rosi, F. Sorrentino, L. Cacciapuoti, M. Prevedelli, and G. M. Tino, Precision measurement of the newtonian gravitational constant using cold atoms, *Nature* **510**, 518 (2014).
- [9] C. L. Garrido Alzar, Compact chip-scale guided cold atom gyrometers for inertial navigation: Enabling technologies and design study, *AVS Quantum Science* **1**, 014702 (2019).
- [10] L. Salvi, N. Poli, V. Vuletić, and G. M. Tino, Squeezing on momentum states for atom interferometry, *Phys. Rev. Lett.* **120**, 033601 (2018).
- [11] S. S. Szigeti, S. P. Nolan, J. D. Close, and S. A. Haine, High-precision quantum-enhanced gravimetry with a Bose-Einstein condensate, *Phys. Rev. Lett.* **125**, 100402 (2020).
- [12] L. I. R. Gil, R. Mukherjee, E. M. Bridge, M. P. A. Jones, and T. Pohl, Spin squeezing in a Rydberg lattice clock, *Phys. Rev. Lett.* **112**, 103601 (2014).
- [13] L. Pezzè and A. Smerzi, Heisenberg-limited noisy atomic clock using a hybrid coherent and squeezed state protocol, *Phys. Rev. Lett.* **125**, 210503 (2020).
- [14] M. Schulte, C. Lisdat, P. O. Schmidt, U. Sterr, and K. Hammerer, Prospects and challenges for squeezing-enhanced optical atomic clocks, *Nat. Commun.* **11**, 5955 (2020).
- [15] B. K. Malia, Y. Wu, J. Martínez-Rincón, and M. A. Kasevich, Distributed quantum sensing with mode-entangled spin-squeezed atomic states, *Nature* **612**, 661 (2022).
- [16] W. J. Eckner, N. D. Oppong, A. Cao, A. W. Young, W. R. Milner, J. M. Robinson, J. Ye, and A. M. Kaufman, Realizing spin squeezing with Rydberg interactions in an optical clock, *Nature* **621**, 734 (2023).
- [17] J. M. Robinson, M. Miklos, Y. M. Tso, C. J. Kennedy, T. Bothwell, D. Kedar, J. K. Thompson, and J. Ye, Direct comparison of two spin-squeezed optical clock ensembles at the 10^{-17} level, *Nature Physics* **20**, 208 (2024).
- [18] W. Muessel, H. Strobel, D. Linnemann, D. B. Hume, and M. K. Oberthaler, Scalable spin squeezing for quantum-enhanced magnetometry with Bose-Einstein condensates, *Phys. Rev. Lett.* **113**, 103004 (2014).
- [19] J. B. Brask, R. Chaves, and J. Kołodyński, Improved quantum magnetometry beyond the standard quantum limit, *Phys. Rev. X* **5**, 031010 (2015).
- [20] H. Bao, J. Duan, S. Jin, X. Lu, P. Li, W. Qu, M. Wang, I. Novikova, E. E. Mikhailov, K.-F. Zhao, K. Mølmer, H. Shen, and Y. Xiao, Spin squeezing of 10^{11} atoms by prediction and retrodiction measurements, *Nature* **581**, 159 (2020).
- [21] C. Troullinou, R. Jiménez-Martínez, J. Kong, V. G. Lucivero, and M. W. Mitchell, Squeezed-light enhancement and backaction evasion in a high sensitivity optically pumped magnetometer, *Phys. Rev. Lett.* **127**, 193601 (2021).
- [22] S. Jin, H. Bao, J. Duan, X. Lu, M. Wang, K.-F. Zhao, H. Shen, and Y. Xiao, Adiabaticity in state preparation for spin squeezing of large atom ensembles, *Photon. Res.* **9**, 2296 (2021).
- [23] J. Kong, R. Jiménez-Martínez, C. Troullinou, V. G.

- Lucivero, G. Tóth, and M. W. Mitchell, Measurement-induced, spatially-extended entanglement in a hot, strongly-interacting atomic system, *Nature Communications* **11**, 2415 (2020).
- [24] X. Wang, A. Miranowicz, Y.-x. Liu, C. P. Sun, and F. Nori, Sudden vanishing of spin squeezing under decoherence, *Phys. Rev. A* **81**, 022106 (2010).
- [25] P. Xue, Spin-squeezing property of weighted graph states, *Phys. Rev. A* **86**, 023812 (2012).
- [26] M. Koppenhöfer and A. A. Clerk, Revisiting the impact of dissipation on time-reversed one-axis-twist quantum-sensing protocols, *Phys. Rev. Res.* **5**, 043279 (2023).
- [27] L. Jiao, W. Wu, S.-Y. Bai, and J.-H. An, Quantum metrology in the noisy intermediate-scale quantum era, *Advanced Quantum Technologies* **n/a**, 2300218.
- [28] M.-Z. Huang, J. A. de la Paz, T. Mazzone, K. Ott, P. Rosenbusch, A. Sinatra, C. L. Garrido Alzar, and J. Reichel, Observing spin-squeezed states under spin-exchange collisions for a second, *PRX Quantum* **4**, 020322 (2023).
- [29] Y. Baamara, A. Sinatra, and M. Gessner, Scaling laws for the sensitivity enhancement of non-Gaussian spin states, *Phys. Rev. Lett.* **127**, 160501 (2021).
- [30] G. Bornet, G. Emperauger, C. Chen, B. Ye, M. Block, M. Bintz, J. A. Boyd, D. Barredo, T. Comparin, F. Mezzacapo, T. Roscilde, T. Lahaye, N. Y. Yao, and A. Browaeys, Scalable spin squeezing in a dipolar Rydberg atom array, *Nature* **621**, 728 (2023).
- [31] T. Roscilde, F. Caleca, A. Angelone, and F. Mezzacapo, Scalable spin squeezing from critical slowing down in short-range interacting systems, *Phys. Rev. Lett.* **133**, 210401 (2024).
- [32] A. Z. Chaudhry and J. Gong, Protecting and enhancing spin squeezing via continuous dynamical decoupling, *Phys. Rev. A* **86**, 012311 (2012).
- [33] X.-P. Liao, M.-S. Rong, and M.-F. Fang, Protecting and enhancing spin squeezing from decoherence using weak measurements, *Laser Physics Letters* **14**, 065201 (2017).
- [34] S.-Y. Bai and J.-H. An, Generating stable spin squeezing by squeezed-reservoir engineering, *Phys. Rev. Lett.* **127**, 083602 (2021).
- [35] A. Rivas, S. F. Huelga, and M. B. Plenio, Quantum non-Markovianity: characterization, quantification and detection, *Reports on Progress in Physics* **77**, 094001 (2014).
- [36] H.-P. Breuer, E.-M. Laine, J. Piilo, and B. Vacchini, Colloquium: Non-Markovian dynamics in open quantum systems, *Rev. Mod. Phys.* **88**, 021002 (2016).
- [37] I. de Vega and D. Alonso, Dynamics of non-Markovian open quantum systems, *Rev. Mod. Phys.* **89**, 015001 (2017).
- [38] L. Li, M. J. Hall, and H. M. Wiseman, Concepts of quantum non-Markovianity: A hierarchy, *Physics Reports* **759**, 1 (2018).
- [39] K. Bai, Z. Peng, H.-G. Luo, and J.-H. An, Retrieving ideal precision in noisy quantum optical metrology, *Phys. Rev. Lett.* **123**, 040402 (2019).
- [40] A. W. Chin, S. F. Huelga, and M. B. Plenio, Quantum metrology in non-Markovian environments, *Phys. Rev. Lett.* **109**, 233601 (2012).
- [41] X. Long, W.-T. He, N.-N. Zhang, K. Tang, Z. Lin, H. Liu, X. Nie, G. Feng, J. Li, T. Xin, Q. Ai, and D. Lu, Entanglement-enhanced quantum metrology in colored noise by quantum Zeno effect, *Phys. Rev. Lett.* **129**, 070502 (2022).
- [42] S.-Y. Bai and J.-H. An, Floquet engineering to overcome no-go theorem of noisy quantum metrology, *Phys. Rev. Lett.* **131**, 050801 (2023).
- [43] W. M. Itano, J. C. Bergquist, J. J. Bollinger, J. M. Gilligan, D. J. Heinzen, F. L. Moore, M. G. Raizen, and D. J. Wineland, Quantum projection noise: Population fluctuations in two-level systems, *Phys. Rev. A* **47**, 3554 (1993).
- [44] B. C. Sanders, Quantum dynamics of the nonlinear rotator and the effects of continual spin measurement, *Phys. Rev. A* **40**, 2417 (1989).
- [45] L.-N. Wu, G.-R. Jin, and L. You, Spin squeezing of the non-Hermitian one-axis twisting model, *Phys. Rev. A* **92**, 033826 (2015).
- [46] A. Fujiwara, Quantum channel identification problem, *Phys. Rev. A* **63**, 042304 (2001).
- [47] T. Fernholz, H. Krauter, K. Jensen, J. F. Sherson, A. S. Sørensen, and E. S. Polzik, Spin squeezing of atomic ensembles via nuclear-electronic spin entanglement, *Phys. Rev. Lett.* **101**, 073601 (2008).
- [48] S. Chaudhury, S. Merkel, T. Herr, A. Silberfarb, I. H. Deutsch, and P. S. Jessen, Quantum control of the hyperfine spin of a Cs atom ensemble, *Phys. Rev. Lett.* **99**, 163002 (2007).
- [49] J. Grond, J. Schmiedmayer, and U. Hohenester, Optimizing number squeezing when splitting a mesoscopic condensate, *Phys. Rev. A* **79**, 021603 (2009).
- [50] C. Orzel, A. K. Tuchman, M. L. Fenselau, M. Yasuda, and M. A. Kasevich, Squeezed states in a Bose-Einstein condensate, *Science* **291**, 2386 (2001).
- [51] K. Helmerson and L. You, Creating massive entanglement of Bose-Einstein condensed atoms, *Phys. Rev. Lett.* **87**, 170402 (2001).
- [52] J. G. Bohnet, B. C. Sawyer, J. W. Britton, M. L. Wall, A. M. Rey, M. Foss-Feig, and J. J. Bollinger, Quantum spin dynamics and entanglement generation with hundreds of trapped ions, *Science* **352**, 1297 (2016).
- [53] Y. Lu, S. Zhang, K. Zhang, W. Chen, Y. Shen, J. Zhang, J.-N. Zhang, and K. Kim, Global entangling gates on arbitrary ion qubits, *Nature* **572**, 363 (2019).
- [54] C. Figgatt, A. Ostrander, N. M. Linke, K. A. Landsman, D. Zhu, D. Maslov, and C. Monroe, Parallel entangling operations on a universal ion-trap quantum computer, *Nature* **572**, 368 (2019).
- [55] C. Song, K. Xu, W. Liu, C.-p. Yang, S.-B. Zheng, H. Deng, Q. Xie, K. Huang, Q. Guo, L. Zhang, P. Zhang, D. Xu, D. Zheng, X. Zhu, H. Wang, Y.-A. Chen, C.-Y. Lu, S. Han, and J.-W. Pan, 10-qubit entanglement and parallel logic operations with a superconducting circuit, *Phys. Rev. Lett.* **119**, 180511 (2017).
- [56] C. Song, K. Xu, H. Li, Y.-R. Zhang, X. Zhang, W. Liu, Q. Guo, Z. Wang, W. Ren, J. Hao, H. Feng, H. Fan, D. Zheng, D.-W. Wang, H. Wang, and S.-Y. Zhu, Generation of multicomponent atomic Schrödinger cat states of up to 20 qubits, *Science* **365**, 574 (2019).
- [57] K. Xu, Z.-H. Sun, W. Liu, Y.-R. Zhang, H. Li, H. Dong, W. Ren, P. Zhang, F. Nori, D. Zheng, H. Fan, and H. Wang, Probing dynamical phase transitions with a superconducting quantum simulator, *Science Advances* **6**, eaba4935 (2020).
- [58] Y. C. Liu, Z. F. Xu, G. R. Jin, and L. You, Spin squeezing: Transforming one-axis twisting into two-axis twisting, *Phys. Rev. Lett.* **107**, 013601 (2011).
- [59] J.-Y. Zhang, X.-F. Zhou, G.-C. Guo, and Z.-W. Zhou,

- Dynamical spin squeezing via a higher-order Trotter-Suzuki approximation, *Phys. Rev. A* **90**, 013604 (2014).
- [60] W. Huang, Y.-L. Zhang, C.-L. Zou, X.-B. Zou, and G.-C. Guo, Two-axis spin squeezing of two-component Bose-Einstein condensates via continuous driving, *Phys. Rev. A* **91**, 043642 (2015).
- [61] L.-G. Huang, X. Zhang, Y. Wang, Z. Hua, Y. Tang, and Y.-C. Liu, Heisenberg-limited spin squeezing in coupled spin systems, *Phys. Rev. A* **107**, 042613 (2023).
- [62] P. Xu, H. Sun, S. Yi, and W. Zhang, Rebuilding of destroyed spin squeezing in noisy environments, *Sci. Rep.* **7**, 14102 (2017).
- [63] Q.-J. Tong, J.-H. An, H.-G. Luo, and C. H. Oh, Mechanism of entanglement preservation, *Phys. Rev. A* **81**, 052330 (2010).
- [64] W.-M. Zhang, P.-Y. Lo, H.-N. Xiong, M. W.-Y. Tu, and F. Nori, General non-Markovian dynamics of open quantum systems, *Phys. Rev. Lett.* **109**, 170402 (2012).
- [65] H.-J. Zhu, G.-F. Zhang, L. Zhuang, and W.-M. Liu, Universal dissipationless dynamics in Gaussian continuous-variable open systems, *Phys. Rev. Lett.* **121**, 220403 (2018).
- [66] K. Kraus, A. Böhm, J. D. Dollard, and W. H. Wootters, *States, Effects, and Operations Fundamental Notions of Quantum Theory: Lectures in Mathematical Physics at the University of Texas at Austin* (Springer Berlin Heidelberg, Berlin, Heidelberg, 1983).
- [67] See the Supplemental Material for the derivation of dynamical solution and its long-time limit, the spin squeezing parameter, and the Husimi Q function.
- [68] U. Dorner, R. Demkowicz-Dobrzanski, B. J. Smith, J. S. Lundeen, W. Wasilewski, K. Banaszek, and I. A. Walmsley, Optimal quantum phase estimation, *Phys. Rev. Lett.* **102**, 040403 (2009).
- [69] J. J. Cooper, D. W. Hallwood, J. A. Dunningham, and J. Brand, Robust quantum enhanced phase estimation in a multimode interferometer, *Phys. Rev. Lett.* **108**, 130402 (2012).
- [70] Z. Huang, K. R. Motes, P. M. Anisimov, J. P. Dowling, and D. W. Berry, Adaptive phase estimation with two-mode squeezed vacuum and parity measurement, *Phys. Rev. A* **95**, 053837 (2017).
- [71] P. A. Knott, T. J. Proctor, K. Nemoto, J. A. Dunningham, and W. J. Munro, Effect of multimode entanglement on lossy optical quantum metrology, *Phys. Rev. A* **90**, 033846 (2014).
- [72] Y. Liu and A. A. Houck, Quantum electrodynamics near a photonic bandgap, *Nat. Phys.* **13**, 48 (2012).
- [73] L. Krinner, M. Stewart, A. Pazmiño, J. Kwon, and D. Schneble, Spontaneous emission of matter waves from a tunable open quantum system, *Nature* **559**, 589 (2018).
- [74] J. Kwon, Y. Kim, A. Lanuza, and D. Schneble, Formation of matter-wave polaritons in an optical lattice, *Nature Physics* **18**, 657 (2022).
- [75] Y. Kim, A. Lanuza, and D. Schneble, Super- and subradiant dynamics of quantum emitters mediated by atomic matter waves, *Nature Physics* **21**, 70 (2025).
- [76] O. Hosten, N. J. Engelsen, R. Krishnakumar, and M. A. Kasevich, Measurement noise 100 times lower than the quantum-projection limit using entangled atoms, *Nature* **529**, 505 (2016).
- [77] D. Tamascelli, A. Smirne, S. F. Huelga, and M. B. Plenio, Nonperturbative treatment of non-Markovian dynamics of open quantum systems, *Phys. Rev. Lett.* **120**, 030402 (2018).
- [78] A. Lemmer, C. Cormick, D. Tamascelli, T. Schaetz, S. F. Huelga, and M. B. Plenio, A trapped-ion simulator for spin-boson models with structured environments, *New J. Phys.* **20**, 073002 (2018).
- [79] J. Franke, S. R. Muleady, R. Kaubruegger, F. Kranzl, R. Blatt, A. M. Rey, M. K. Joshi, and C. F. Roos, Quantum-enhanced sensing on optical transitions through finite-range interactions, *Nature* **621**, 740 (2023).
- [80] G.-X. Wang, Y.-K. Wu, R. Yao, W.-Q. Lian, Z.-J. Cheng, Y.-L. Xu, C. Zhang, Y. Jiang, Y.-Z. Xu, B.-X. Qi, P.-Y. Hou, Z.-C. Zhou, L. He, and L.-M. Duan, Simulating the spin-boson model with a controllable reservoir in an ion trap, *Phys. Rev. A* **109**, 062402 (2024).
- [81] C. D. Bruzewicz, R. McConnell, J. Chiaverini, and J. M. Sage, Scalable loading of a two-dimensional trapped-ion array, *Nature Communications* **7**, 13005 (2016).
- [82] P. Xue, Non-Markovian dynamics of spin squeezing, *Physics Letters A* **377**, 1328 (2013).
- [83] J.-Q. Li, L. Du, and J.-Q. Liang, Spin squeezing and pairwise entanglement under non-Markovian environments with dynamical decoupling pulses, *Laser Physics* **28**, 095202 (2018).
- [84] X. Yin, J. Ma, X. Wang, and F. Nori, Spin squeezing under non-Markovian channels by the hierarchy equation method, *Phys. Rev. A* **86**, 012308 (2012).
- [85] Y.-H. Ma, Q.-Z. Ding, and T. Yu, Persistent spin squeezing of a dissipative one-axis twisting model embedded in a general thermal environment, *Phys. Rev. A* **101**, 022327 (2020).

Supplemental Material to “Protecting spin squeezing from decoherence”

Lin Jiao,¹ Han Pu,^{1,*} and Jun-Hong An^{2,†}

¹*Department of Physics and Astronomy, and Smalley-Curl Institute,
Rice University, Houston, TX 77251-1892, USA*

²*Key Laboratory of Quantum Theory and Applications of MoE,
Lanzhou Center for Theoretical Physics, Key Laboratory of Theoretical Physics of Gansu Province,
Gansu Provincial Research Center for Basic Disciplines of Quantum Physics, Lanzhou University, Lanzhou 730000, China*

In this Supplemental Material, we give the detailed derivation of dynamical solution and its long-time limit, the spin squeezing parameter and the Husimi Q function of the evolved states from the initial one- and two-axis twisted states.

I. DYNAMICS

The dynamics of the N spins influenced by N identical dissipative environments is governed by the non-Markovian master equation

$$\dot{\rho}(t) = \sum_{l=1}^N \{-i\Omega(t)[\hat{\sigma}_l^\dagger \hat{\sigma}_l, \rho(t)] + \Gamma(t)\check{\mathcal{L}}_l \rho(t)\}, \quad (\text{S1})$$

where $\check{\mathcal{L}}_l \rho(t) = 2\hat{\sigma}_l \rho(t) \hat{\sigma}_l^\dagger - \{\hat{\sigma}_l^\dagger \hat{\sigma}_l, \rho(t)\}$ is the Lindblad superoperator and $\Gamma(t) + i\Omega(t) = -\dot{u}(t)/u(t)$, with $u(t)$ determined by

$$\dot{u}(t) + i\omega_0 u(t) + \int_0^t d\tau f(t-\tau)u(\tau) = 0, \quad (\text{S2})$$

under $u(0) = 1$. Here, $f(t-\tau) = \int d\omega J(\omega)e^{-i\omega t}$ is the environmental correlation function. In the special case where the spin-environment coupling is weak and the time scale of the environmental correlation function is much smaller than the one of the spins, we can make the Born-Markov approximation by neglecting the memory effect and extending the upper limit of the integral to ∞ [1, 2]. It results in $u_{\text{BMA}}(t) = e^{-[\kappa+i(\omega_0+\Delta(\omega_0))]t}$ with $\kappa = \pi J(\omega_0)$, $\Delta(\omega_0) = \mathcal{P} \int_0^\infty \frac{J(\omega)}{\omega_0 - \omega} d\omega$, and \mathcal{P} being the Cauchy principal value.

In the general non-Markovian case, the analytic expression of Eq. (S2) can be formally obtained by Laplace transform, which convert Eq. (S2) to $\tilde{u}(z) = [z + i\omega_0 + \int \frac{J(\omega)}{z+i\omega} d\omega]^{-1}$. $u(t)$ is just the inverse Laplace transform on $\tilde{u}(z)$, i.e., $u(t) = \frac{1}{2\pi i} \int_{i\sigma+\infty}^{i\sigma-\infty} \tilde{u}(-iE)e^{-iEt} dE$, where σ is larger than any poles of $\tilde{u}(z)$. The poles of $\tilde{u}(z)$ are determined by

$$Y(E) = E, \quad (\text{S3})$$

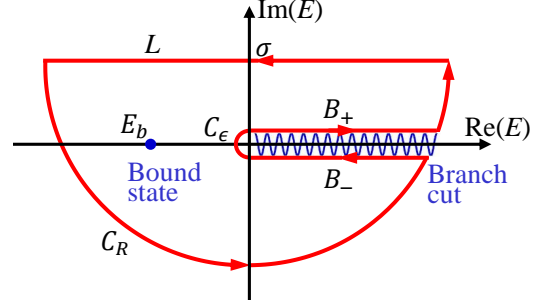


FIG. S1. Path of the contour integration in the $\text{Re}(E)$ - $\text{Im}(E)$ plane for the calculation of the inverse Laplace transform of $\tilde{u}(E)$.

where $Y(E) \equiv \omega_0 - \int_0^\infty \frac{J(\omega)}{\omega - E} d\omega$. It is interesting to note that Eq. (S3) is also the equation of the eigenenergy in the single-excitation subspace of each local spin-environment system. To confirm this, we expand the eigenstate of the l th local system as $|\Phi\rangle = (c\hat{\sigma}_l^\dagger + \sum_k d_k \hat{a}_{lk}^\dagger)|g_l, \{0_k\}\rangle$. Inserting it into the Schrödinger equation $\hat{H}_l|\Phi\rangle = E|\Phi\rangle$, we obtain $E\alpha = \omega_0\alpha + \sum_k g_k \beta_k$ and $E\beta_k = \omega_k \beta_k + g_k^* \alpha$, where E is the eigenenergy. These equations easily lead to Eq. (S3) in the continuum limit of the environmental frequencies. This signifies that the decoherence dynamics of each spin is essentially determined by the energy-spectrum characteristics in the single-excitation subspace of the total spin-environment system. Because $Y(E)$ is decreasing in the region $E < 0$, Eq. (S3) has one isolated root denoted by E_b in this region whenever $Y(0) < 0$, i.e., $\omega_0 < \eta\omega_c\gamma(s)$ for the Ohmic-family spectral density, where $\gamma(s)$ is the Euler gamma function. Due to the singularity in the integral, $Y(E)$ is ill-defined and jumps rapidly between $\pm\infty$ when $E > 0$. Thus, Eq. (S3) has infinite roots in the region $E > 0$, forming a continuous energy band. We call the eigenstate corresponding to the isolated eigenenergy E_b the bound states. According to the path of the contour integration to evaluate the inverse Laplace transform, see Fig. S1, and using the residue theorem, we obtain

$$u(t) = Z e^{-iE_b t} + \int_0^\infty \mathcal{C}(E) e^{-iEt} dE, \quad (\text{S4})$$

where $Z = [1 + \int_0^\infty \frac{J(\omega)d\omega}{(E_b - \omega)^2}]^{-1}$ originates from the residue contributed by the bound state and $\mathcal{C}(E) = J(E)/\{[E - \omega_0 - \Delta(E)]^2 + [\pi J(E)]^2\}$ from the integration paths B_\pm

* hpu@rice.edu

† anjhong@lzu.edu.cn

contributed by the continuum energy band. The second term of Eq. (S4) goes to zero in the long-time limit due to the out-of-phase interference. Thus, we obtain the steady state solution of Eq. (S4) as

$$\lim_{t \rightarrow \infty} u(t) = \begin{cases} 0, & Y(0) \geq 0 \\ Ze^{-iE_b t}, & Y(0) < 0 \end{cases}. \quad (\text{S5})$$

Equation (S5) clearly demonstrates the dominated role of the bound state in the non-Markovian decoherence dynamics of the spin.

If only one spin is contained in the system, then the solution of Eq. (S1) can be easily represented by the Kraus operators as $\rho_{N=1}(t) = \check{\Lambda}_t \rho_{N=1}(0)$, where $\check{\Lambda}_t = \sum_{\mu=1}^2 \hat{K}_\mu(t) \cdot \hat{K}_\mu^\dagger(t)$, $\hat{K}_1 = \text{diag}[u(t), 1]$, and $\hat{K}_2 = [1 - |u(t)|^2]^{1/2} \hat{\sigma}$. Due to the dynamical independence of the N spins in Eq. (S1), its solution for arbitrary N reads $\rho(t) = \check{\Lambda}_t^{\otimes N} \rho(0)$. The expectation value for any operator \hat{O} in $\rho(t)$ can then be recast into

$$\langle \hat{O} \rangle \equiv \text{Tr}[\hat{O} \check{\Lambda}_t \rho(0)] = \langle (\check{\Lambda}_t^\dagger \hat{O}) \rho(0) \rangle \equiv \langle (\check{\Lambda}_t^\dagger \hat{O}) \rangle_0, \quad (\text{S6})$$

which is just the expectation value of $\check{\Lambda}_t^\dagger \hat{O}$ in the initial state $\rho(0)$. This could dramatically facilitate our calculations.

II. SPIN SQUEEZING PARAMETER

Represented by the expectation values of several collective spin operators, the spin squeezing parameter of the state $\rho(t)$ is $\xi \equiv \sqrt{N} \min_\beta \Delta J_{\perp, \beta} / |\langle \hat{\mathbf{J}} \rangle|$, where $\Delta J_{\perp, \beta} = (\langle \hat{J}_{\perp, \beta}^2 \rangle - \langle \hat{J}_{\perp, \beta} \rangle^2)^{1/2}$ is the uncertainty of $\hat{J}_{\perp, \beta} = (\cos \beta \mathbf{n}_1 + \sin \beta \mathbf{n}_2) \cdot \hat{\mathbf{J}}$, with $\mathbf{n}_{1,2}$ being two orthogonal unit vectors perpendicular to the mean spin direction \mathbf{n}_0 [3]. According to Eq. (S6), the expectation values of these operators in $\rho(t)$ are converted into the ones of their corresponding inversely evolved operators in $\rho(0)$.

First, we consider the spin squeezed states from one-axis twisting model

$$|\Psi_{\text{OAT}}\rangle = e^{-i\Theta \hat{J}_x^2} |j, -j\rangle, \quad (\text{S7})$$

with $j = N/2$ and $|j, -j\rangle$ is the common eigenstate of \hat{J}^2 and \hat{J}_z , as the initial states. Both $|\Psi_{\text{OAT}}\rangle$ and its evolved state $\rho(t)$ are invariant under the permutation of the constitute spins. Therefore, the expectation values of the collective spin operators satisfy [4]

$$\langle \hat{J}_\alpha \rangle = N \langle \hat{\sigma}_1^\alpha \rangle / 2 = N \langle \check{\Lambda}_t^\dagger \hat{\sigma}_1^\alpha \rangle_0 / 2. \quad (\text{S8})$$

The Kraus representation of $\check{\Lambda}_t$ gives

$$\check{\Lambda}_t^\dagger \hat{\sigma}_1 = u(t) \hat{\sigma}_1, \quad (\text{S9})$$

$$\check{\Lambda}_t^\dagger \hat{\sigma}_1^z = |u(t)|^2 \hat{\sigma}_1^z - 1 + |u(t)|^2, \quad (\text{S10})$$

where $\hat{\sigma} = (\hat{\sigma}^x - i\hat{\sigma}^y)/2$. It is straightforward to calculate $\langle \hat{\sigma}_1 \rangle_0 = 0$, which causes $\langle \hat{\sigma}_1^x \rangle_0 = \langle \hat{\sigma}_1^y \rangle_0 = 0$, and $\langle \hat{\sigma}_1^z \rangle_0 = -\cos^2 \Theta$ for $|\Psi_{\text{OAT}}\rangle$. Then the mean spin is

$$\langle \hat{\mathbf{J}} \rangle = \frac{N}{2} [|u(t)|^2 (1 - \cos^2 \Theta) - 1] (0, 0, 1). \quad (\text{S11})$$

The concerned spin component in ξ perpendicular to $\langle \hat{\mathbf{J}} \rangle$ becomes $\hat{J}_{\perp, \beta} = \cos \beta \hat{J}_y + \sin \beta \hat{J}_z$. Its minimal uncertainty optimizing all β reads

$$\min_\beta \Delta J_{\perp, \beta}^2 = (\langle \hat{J}_x^2 + \hat{J}_y^2 \rangle - |\langle \hat{J}_- \rangle|^2) / 2, \quad (\text{S12})$$

where $\hat{J}_- = \hat{J}_x - i\hat{J}_y$. To calculate the expectation values of the squared spin operators, we again use the permutation symmetry and obtain

$$\begin{aligned} \langle \hat{J}_\alpha^2 \rangle &= N[1 + (N-1) \langle \hat{\sigma}_1^\alpha \hat{\sigma}_2^\alpha \rangle] / 4, \\ &= N[1 + (N-1) \langle (\check{\Lambda}_t^\dagger \hat{\sigma}_1^\alpha) (\check{\Lambda}_t^\dagger \hat{\sigma}_2^\alpha) \rangle_0] / 4, \end{aligned} \quad (\text{S13})$$

$$\begin{aligned} \langle \hat{J}_-^2 \rangle &= N(N-1) \langle \hat{\sigma}_1 \hat{\sigma}_2 \rangle \\ &= N(N-1) \langle (\check{\Lambda}_t^\dagger \hat{\sigma}_1) (\check{\Lambda}_t^\dagger \hat{\sigma}_2) \rangle_0. \end{aligned} \quad (\text{S14})$$

The Kraus representations in Eqs. (S9) and (S10) give

$$\begin{aligned} &\langle (\check{\Lambda}_t^\dagger \hat{\sigma}_1^x) (\check{\Lambda}_t^\dagger \hat{\sigma}_2^x) \rangle_0 + \langle (\check{\Lambda}_t^\dagger \hat{\sigma}_1^y) (\check{\Lambda}_t^\dagger \hat{\sigma}_2^y) \rangle_0 \\ &= 2|u(t)|^2 \langle \hat{\sigma}_1 \hat{\sigma}_2 \rangle_0 + \text{c.c.}, \end{aligned} \quad (\text{S15})$$

$$\langle (\check{\Lambda}_t^\dagger \hat{\sigma}_1) (\check{\Lambda}_t^\dagger \hat{\sigma}_2) \rangle_0 = u(t)^2 \langle \hat{\sigma}_1 \hat{\sigma}_2 \rangle_0. \quad (\text{S16})$$

One can easily calculate $\langle \hat{\sigma}_1 \hat{\sigma}_2^j \rangle_0 = A/8$ and $\langle \hat{\sigma}_1 \hat{\sigma}_2 \rangle_0 = -(A - iB)/8$, with $A = 1 - \cos^{N-2}(2\Theta)$ and $B = 4 \sin \Theta \cos^{N-2} \Theta$, for $|\Psi_{\text{OAT}}\rangle$. Substituting Eqs. (S15) and (S16) in Eqs. (S13) and (S14), we have

$$\min_\beta \Delta J_{\perp, \beta}^2 = \frac{N}{4} \left[1 + \frac{(N-1)|u(t)|^2}{4} (A - \sqrt{A^2 + B^2}) \right]. \quad (\text{S17})$$

Therefore, we finally derive the spin squeezing parameter

$$\xi_{\text{OAT}}^2(t) \simeq 1 + (N-1)|u(t)|^2 (A - \sqrt{A^2 + B^2}) / 4 \quad (\text{S18})$$

for the evolved state from the initial state $|\Psi_{\text{OAT}}\rangle$. Accompanying the formation of the bound state, the non-Markovian dynamics leads Eq. (S18) to the steady-state value

$$\xi_{\text{OAT}}^2(\infty) \simeq 1 + (N-1)Z^2 (A - \sqrt{A^2 + B^2}) / 4. \quad (\text{S19})$$

Expanding it in the large N and small Θ limit, i.e., $N\Theta^2 \ll 1 \ll N\Theta$, we have [5]

$$\xi_{\text{OAT}}^2(\infty) \simeq 1 + Z^2 (N^{-2} \Theta^{-2} + N^2 \Theta^4 / 6 - 1), \quad (\text{S20})$$

which attains its minimum $\xi_{\text{OAT}}^2(\infty)|_{\Theta=\Theta_0} \simeq 1.04Z^2 N^{-\frac{2}{3}} + 1 - Z^2$ at $\Theta = 3^{1/6} N^{2/3} \equiv \Theta_0$. In the large N limit, we obtain the same N -scaling as in the ideal decoherence-free case.

Second, we consider the spin squeezed state from the two-axis twisting model

$$|\Psi_{\text{TAT}}\rangle = e^{i\Theta(\hat{J}_+^2 - \hat{J}_-^2)} |j, -j\rangle \quad (\text{S21})$$

as the initial state. It also possesses the permutation symmetry, which enables the calculation of $\langle \hat{J}_\alpha \rangle$ from Eqs. (S8), (S9), and (S10). The mean spin is

$$\langle \hat{\mathbf{J}} \rangle = -\frac{N}{2}(0, 0, 1). \quad (\text{S22})$$

Thus, the minimal uncertainty in the plane perpendicular to $\langle \hat{\mathbf{J}} \rangle$ for the evolved state from the initial two-axis twisted state is the same as the one in Eq. (S12) for the one-axis twisted state. The use of the bipartite expansion of the expectation values of the squared spin operators in Eqs. (S13) and (S14) and the Kraus representations in Eqs. (S15) and (S16) results in

$$\langle \hat{J}_x^2 + \hat{J}_y^2 \rangle = \frac{N[1 - |u(t)|^2]}{2} + |u(t)|^2 \langle \hat{J}_x^2 + \hat{J}_y^2 \rangle_0 \quad (\text{S23})$$

$$\langle \hat{J}_-^2 \rangle = u(t)^2 \langle \hat{J}_-^2 \rangle_0, \quad (\text{S24})$$

where the initial conditions $\langle \hat{\sigma}_1 \hat{\sigma}_2^\dagger + \hat{\sigma}_2 \hat{\sigma}_1^\dagger \rangle_0 = [2\langle \hat{J}_x^2 + \hat{J}_y^2 \rangle_0 / N - 1] / (N - 1)$ and $\langle \hat{\sigma}_1 \hat{\sigma}_2 \rangle_0 = \langle \hat{J}_-^2 \rangle_0 / [N(N - 1)]$ from Eqs. (S13) and (S14) have been used. Then the spin squeezing parameter becomes

$$\xi_{\text{TAT}}^2(t) = 1 - |u(t)|^2 + \frac{2|u(t)|^2}{N} [|\langle \hat{J}_x^2 + \hat{J}_y^2 \rangle_0 - |\langle \hat{J}_-^2 \rangle_0|], \quad (\text{S25})$$

which is Eq. (12) of the main text. Unlike the one-axis twisted case, here analytical expressions for $\langle \hat{J}_x^2 + \hat{J}_y^2 \rangle_0$ and $\langle \hat{J}_-^2 \rangle_0$ cannot be obtained.

III. HUSIMI Q FUNCTION

The spin coherent state is

$$|\theta, \varphi\rangle = \frac{e^{\zeta \hat{J}_-}}{(1 + |\zeta|^2)^j} |j, j\rangle = [\cos \frac{\theta}{2} |e\rangle + e^{i\varphi} \sin \frac{\theta}{2} |g\rangle]^{\otimes N}, \quad (\text{S26})$$

where $\zeta = e^{i\varphi} \tan \frac{\theta}{2}$. The Husimi Q function for the state $\rho(t)$ of the spin system is defined as

$$\begin{aligned} Q(\theta, \varphi) &= \frac{2j+1}{4\pi} \text{Tr}[\rho(t) |\theta, \varphi\rangle \langle \theta, \varphi|] \\ &= \frac{2j+1}{4\pi} \langle \Lambda_t^{\dagger \otimes N} |\theta, \varphi\rangle \langle \theta, \varphi| \rangle_0, \end{aligned} \quad (\text{S27})$$

which maps $\rho(t)$ to a quasiclassical probability distribution in the phase space defined by the spin coherent state $|\theta, \varphi\rangle$. Rewriting Eq. (S26) as

$$|\theta, \varphi\rangle \langle \theta, \varphi| = \left[\frac{I}{2} + \frac{\cos \theta}{2} \hat{\sigma}^z + \frac{\sin \theta}{2} (e^{i\varphi} \hat{\sigma} + \text{h.c.}) \right]^{\otimes N}, \quad (\text{S28})$$

we obtain

$$\begin{aligned} Q(\theta, \varphi) &= \frac{2j+1}{4\pi} \left\langle \left[\frac{I}{2} + \frac{\cos \theta}{2} \check{\Lambda}_t^\dagger \hat{\sigma}^z \right. \right. \\ &\quad \left. \left. + \frac{\sin \theta}{2} (e^{i\varphi} \check{\Lambda}_t^\dagger \hat{\sigma} + \text{h.c.}) \right]^{\otimes N} \right\rangle_0. \end{aligned} \quad (\text{S29})$$

Substituting the Kraus representations in Eqs. (S15) and (S16) into Eq. (S29), the Husimi Q function of the evolved states from the initial one- and two-axis twisted states can be numerically calculated for given N .

[1] U. Dorner, R. Demkowicz-Dobrzanski, B. J. Smith, J. S. Lundeen, W. Wasilewski, K. Banaszek, and I. A. Walmsley, Optimal quantum phase estimation, *Phys. Rev. Lett.* **102**, 040403 (2009).
 [2] J. J. Cooper, D. W. Hallwood, J. A. Dunningham, and J. Brand, Robust quantum enhanced phase estimation in a multimode interferometer, *Phys. Rev. Lett.* **108**, 130402 (2012).

[3] D. J. Wineland, J. J. Bollinger, W. M. Itano, and D. J. Heinzen, Squeezed atomic states and projection noise in spectroscopy, *Phys. Rev. A* **50**, 67 (1994).
 [4] J. Ma, X. Wang, C. Sun, and F. Nori, Quantum spin squeezing, *Physics Reports* **509**, 89 (2011).
 [5] M. Kitagawa and M. Ueda, Squeezed spin states, *Phys. Rev. A* **47**, 5138 (1993).